

OPT is a microscopic imaging technique for obtaining three-dimensional, reconstructed images of small biological samples (16). The principle of OPT is that the light passes through the specimen labeled and cleared for a standard back-projection algorithm to generate a relatively high resolution tomographic image. A three-dimensional image of the specimen is reconstructed using the individual tomographic images. The advantage of OPT is the capability to investigate spatial distribution of such target molecules as RNA and protein without slicing of the target organs, and at a higher resolution.

In this report, we show that the number and volume of intraportally transplanted islets in liver can be investigated by OPT analysis. In addition, comparing syngeneic and allogeneic rodent islet transplantation models, we demonstrate that the number and volume of transplanted islets is considerably more decreased in allogeneic islet transplantation than in syngeneic transplantation. Thus, *ex vivo* imaging of intraportal islet transplant by OPT may be a useful tool for evaluation and improvement of islet transplantation outcome.

2. Materials and methods

2.1 Animals

Male C57BL/6 Cr Slc mice (Shimizu Laboratory Supplies co. ltd, Japan) aged 8-10 weeks were used as recipients and donors and male BALB/c mice (Shimizu Laboratory Supplies co. ltd, Japan) aged 8 weeks were used as recipients for allogeneic

transplantation. All experiments were approved by the Kyoto University Animal Care Committee.

2.2 Islet isolation and islet transplantation

Islets were isolated from mouse pancreas using collagenase digestion method (17); 3-4 mL Hank's Balanced Salt Solution (HBSS) containing 0.5 mg/mL collagenase (Nitta gelatin, Japan) was infused through the common bile duct. The pancreas was dissected and digested at 37°C for 21 minutes. Islets were separated from exocrine cells by centrifugation with Ficoll-Conray gradient solution for 10 minutes. Diabetes was rendered by a single intraperitoneal injection of streptozotocin (STZ) (Nacalai tesque, Japan), 120 mg/kg body weight, freshly dissolved in 10 mM citrate buffer (pH 4.5)). These mice were used as diabetic recipients if the blood glucose concentration was more than 20 mmol/L on two consecutive days. Recipient mice were anesthetized by isoflurane (Forane, Abbott, Japan) during transplantation. Fresh islets in a volume of about 400 μ L HBSS were injected into the portal vein and transplanted into the right hepatic lobe as previously reported (18). For validation of the OPT method, 75, 150 or 300 islets were transplanted into the right hepatic lobe, which was dissected immediately after transplantation. For comparison of syngeneic and allogeneic transplantation, C57BL/6 mice (H-2^b) were used as recipients; 300 islets isolated from C57BL/6 mice or Balb/c mice (H-2^d) were transplanted, respectively. The blood glucose concentration was determined by glucose meter (Glucocard, Arkley, Japan).

2.3 Tissue preparation and immunostaining

Mice with transplanted islets were sacrificed by cervical dislocation. The transplanted right hepatic lobes were dissected clean and immediately immersed for fixation in 4% paraformaldehyde in PBS for 3 h at 4°C. The fixed samples were washed in PBS, and then transferred stepwise to 100% methanol (MeOH) and stored at -20°C. The immunostaining was performed according to the previous report (19) as follows. The right hepatic lobe was immersed in 15% H₂O₂, 16.7% DMSO solution in MeOH for 24 h to bleach pigmented cells and to reduce auto fluorescence. The liver then was washed in MeOH, which was repeated five times, and then kept at -80°C for at least 1 h before return to room temperature. The organ was rehydrated by TBST (0.15 M NaCl (Nacalai tesque, Japan), 0.1 M Tris(hydroxymethyl)aminomethane (Nacalai tesque, Japan) pH7.4, and 0.1% Triton X-100 (Nacalai tesque, Japan)). TBST containing 10% normal goat serum (Dako) and 0.01% sodium azide (Nacalai tesque, Japan) was used as blocking solution for 24 h. The organ was incubated in insulin antibody (Santacruz CA, USA) in 5% DMSO containing blocking solution for 48 h. After washing, Alexa594 goat anti rabbit IgG (Invitrogen, Carlsbad, CA, USA) was used as secondary antibody for 48 h.

2.4 Optical Projection Tomography (OPT) and image reconstruction

For the observations, the immunostained liver was embedded in 1% agarose gel (low melting point agarose; Sigma Aldrich) to fix the sample. OPT was performed using an OPT scanner (OPT scanner 3001, Bioptonics, UK) according to the manufacturer's instructions (16, 19). The specimens were maintained within the BABB, rotated to a series of angular positions (0.9° apart), and images were captured at each orientation. High-resolution_{al} tomographic images were reconstructed from raw images by NRecon

software (SKYSCAN, Kontich, Belgium). The tomographic images obtained from OPT were reconstructed to three-dimensional form and analyzed by Avizo software (Visualization Science Group, Inc. MA, USA). Three-dimensional images of islets and liver were obtained by isosurface treatment. Total volume of all islets was calculated by summation of the selected islets.

2.5 Statistical analysis

Data and graph were presented as medians (interquartile range), and statistical analysis was performed with Mann-Whitney's U-test. *p* value of less than 0.05 was considered significant.

3. Results

3.1 Observation of transplanted islets in liver by OPT

Transparency of the liver and immunostaining of transplanted islets without sectioning were achieved by the preparation protocols. Figure 1a is a raw OPT image of liver; the insulin-stained transplanted islets are seen as dots in the high magnification image (Figure 1b, white arrows). One of the tomographic images obtained is shown in Figure 1c. Vertically reconstructed images are shown in Figure 1d and 1e, and islets pointed out by arrow and arrowhead in Figure 1c are located as in Figures 1d and 1e, respectively. Some islets appear to be located at the terminal end of the portal vein (Figure 1c and d), and other islets are located at the wall of the proximal branch of the portal vein (Figure 1e). Figure 1f is the reconstructed target-specific image of an islet (arrowhead in Figure 1e) and portal vein. Thus, a three-dimensional image as well as the

size and location of transplanted islets in liver can be investigated (Figure 1g, h. and *Supplementary movie*).

3.2 Evaluation of the effectiveness of OPT analysis of transplanted islets in liver

To correlate the number of islets transplanted and the number of islets detected by OPT, we resected and fixed livers immediately after transplantation of a range of numbers of islets. The three-dimensional reconstructed image shows that the number of spots indicating transplanted islets in the right hepatic lobes was increased in accord with the increased dosage (Figure 2a-c); these numbers are well correlated ($r^2=0.9561$) (Figure 2d). These findings indicate that OPT can be used for quantitative analysis of islets transplanted into liver.

3.3 OPT analysis of islet grafts under syngeneic and allogeneic conditions

To evaluate the time course of transplanted islets in syngeneic and allogeneic conditions, we analyzed the number and volume of islets intraportally transplanted in liver of STZ-induced diabetic mice. Blood glucose concentrations under both syngeneic and allogeneic conditions were normoglycemic until a week after transplantation. However, blood glucose concentrations under allogeneic conditions thereafter became hyperglycemic, while those under syngeneic conditions remained normoglycemic (Figure 3a). The islet-containing livers were resected on day 11 for analysis by OPT method. The number of islets in the syngeneic condition was dramatically greater than that in the allogeneic condition (52 (IQR 16.5) vs 203 (28.5), respectively, $p<0.05$) (Figure 3b).

In OPT-detected islets classified by size, the number in each category was significantly greater in syngeneic than in allogeneic conditions, and showed a similar histogram pattern (Figure 4a). Total volume of islets in syngeneic condition was dramatically greater than that in allogeneic condition (8.6 (2.7) vs. 35.3 (10.1) ($\mu\text{m}^3 \times 10^6$)), respectively, $p < 0.05$) (Figure 4b).

Discussion

In the present study, we demonstrate that islets transplanted intraportally in liver can be analyzed at the cellular level by OPT method, which permits three-dimensional analysis of the distribution of the islets in the liver. Comparing syngeneic and allogeneic islet transplantation models, we show by OPT that the volume of transplanted islets differs significantly at the cellular level.

One of main problems in clinical islet transplantation, poor long-term achievement of insulin independence, is primarily due to graft loss caused by various stressors upon transplantation (4). When islets are injected intraportally, each of them is thought to locate at the respective branched end of the portal vein in liver. In modalities such as BLI, MRI, and PET, only PET allows quantification of graft volume, but the resolution is still too low for detailed analysis of the transplanted islets. On the other hand, while the resolution of conventional immunohistochemistry is high, only restricted slices of the engrafted organ can be analyzed by this method.

OPT, a newly developed method, is reported to permit analysis of a sample at resolution as high as 5 μm . Recently, T. Alanentalo et al. performed detailed analysis of

NOD mice during progression of type 1 diabetes, and showed that a reduction in volume of native islets in pancreas could be detected and quantified by the OPT method (20). We have used OPT method for the first time in the intraportal islet transplantation model and confirm the efficacy of this method of islet imaging (Figures 1 and 2).

However, there are several limitations in use of the OPT method. It can be performed only *ex vivo*, and non-invasive, repeated observation is not possible. In this context, PET and MRI are suitable for *in vivo*, repeated monitoring of transplanted islets. In addition, the maximum sample size for analysis using OPT is about 2 cm. The OPT method also is not clinically applicable as it would require a large liver biopsy.

The OPT method is useful for evaluating small organs of small animals such as rodents, as in our present study. Indeed, using rodent islet transplantation models, the OPT method clearly shows quantitative difference of grafts in liver in syngeneic and allogeneic conditions. In this investigation, the OPT method revealed that 83% of the transplanted islets were lost in the allogeneic condition while about 70% were preserved in the syngeneic condition. Moreover, calculated beta-cell volume in the allogeneic condition was significantly reduced to 24.2% of that in the syngeneic condition (Figures 3b and 4b). This remarkable graft loss by allogeneic immune reaction seems not to be related to the size of the islet graft, as there was no difference in size distribution histogram between the two conditions (Figure 4a). The OPT method also clearly shows the sites where islets adhere and are engrafted in the portal vein. Further investigation is required to determine the effect of islet location on islet engraftment.

In conclusion, we have constructed three-dimensional images of transplanted islets in liver by an OPT method that permits detailed analysis of transplanted islets in liver. This method should be useful for islet transplantation study.

ACKNOWLEDGMENT

This work was supported by a Research Grant from the Ministry of Health, Labour, and Welfare of Japan, and from the Ministry of Education, Culture, Sports, Science, and Technology of Japan, and the Program for Promotion of Fundamental Studies in Health Sciences of the National Institute of Biomedical Innovation (NIBIO), and also by Kyoto University Global COE Program “Center for Frontier Medicine”.

REFERENCES

- (1) Shapiro AM, Lakey JR, Ryan EA, et al. Islet transplantation in seven patients with type 1 diabetes mellitus using a glucocorticoid-free immunosuppressive regimen. *N Engl J Med.* 2000; **343**: 230.
- (2) Shapiro AM, Ricordi C, Hering B. Edmonton's islet success has indeed been replicated elsewhere. *Lancet* 2003; **362**: 1242.
- (3) Ryan EA, Paty BW, Senior PA, et al. Five-year follow-up after clinical islet transplantation. *Diabetes* 2005; **54**: 2060.
- (4) Ricordi C, Strom T. Clinical islet transplantation: advances and immunological challenges. *Nat Rev Immunol* 2004; **4**: 259.
- (5) Lu Y, Dang H, Middleton B, et al. Bioluminescent Monitoring of Islet Graft Survival after Transplantation. *Molecular Therapy* 2004; **9**: 428.
- (6) Fowler M, Virostko J, Chen Z, et al. Assessment of pancreatic islet volume after islet transplantation using in vivo bioluminescence imaging. *Transplantation* 2005; **79**: 768.
- (7) Chen X, Zhang X, Larson CS, Baker MS, Kaufman DB, In vivo bioluminescence imaging of transplanted islets and early detection of graft rejection. *Transplantation* 2006; **81**: 1421.
- (8) Evgenov NV, Medarova Z, Guangping D, Bonner-Weir S, Moore A. *In vivo* imaging of islet transplantation. *Nat Med* 2006; **12**: 144.

- (9) Evgenov NV, Medarova Z, Pratt J, Pantazopoulos P, Leyting S, Bonner-Weir S, Moore A. In vivo imaging of immune rejection in transplanted pancreatic islets. *Diabetes* 2006; **55**: 2419.
- (10) Tai JH, Foster P, Rosales A, et al. White. Imaging Islets Labeled With Magnetic Nanoparticles at 1.5 Tesla. *Diabetes* 2006; **55**: 2931.
- (11) Saudek F, Jiráček D, Girman P, et al. Magnetic resonance imaging of pancreatic islets transplanted into the liver in humans. *Transplantation* 2010; **90**: 1602.
- (12) Lu Y, Dang H, Middleton B, et al. Noninvasive imaging of islet grafts using positron-emission tomography. *Proc Natl Acad Sci USA* 2006; **103**: 11294.
- (13) Toso C, Zaidi H, Morel P, et al. Positron-emission tomography imaging of early events after transplantation of islets of Langerhans. *Transplantation* 2005; **79**: 353.
- (14) Kim SJ, Doudet DJ, Studenov AR, et al. Quantitative micro positron emission tomography (PET) imaging for the *in vivo* determination of pancreatic islet graft survival. *Nat Med* 2006; **12**: 1423.
- (15) Miller K, Kim A, Kilimnik G, Jo J, et al. Islet formation during the neonatal development in mice. *PLoS One* 2009; **4**: e7739.
- (16) Sharpe J, Ahlgren U, Perry P, et al. Optical Projection Tomography as a Tool for 3D Microscopy and Gene Expression Studies. *Science* 2002; **296**: 541.
- (17) Sutton R, Peters M, Mcshane P, Gray DWR, Morris PJ. Isolation of rat pancreatic-islets by ductal injection of collagenase. *Transplantation* 1986; **42**: 689.
- (18) Yonekawa Y, Okitsu T, Wako K, et al. A new mouse model for intraportal islet transplantation with limited hepatic lobe as a graft site. *Transplantation* 2006; **82**: 712.

- (19) Alanentalo T, Asayesh A, Morrison H, et al. Tomographic molecular imaging and 3D quantification within adult mouse organs. *Nat. Methods* 2007; **4**: 31.
- (20) Alanentalo T, Hornblad A, Mayans S, et al. Quantification and Three-Dimensional Imaging of the Insulinitis-Induced Destruction of β -Cells in Murine Type 1 Diabetes. *Diabetes* 2010; **59**: 1756.

Figure Captions

Figure 1. OPT images of liver containing intraportally transplanted islets.

(a) Raw image of islet-transplanted right hepatic lobe, (b) high magnification image (in square of (a)), (c) representative slice image of the transplanted right hepatic lobe; (d), (e) vertical slice image of islet with arrow in (c), arrowhead in (c), respectively. (f) Reconstructed three-dimensional image of islet (in (c) and (e), arrowhead) and portal branch. Three-dimensional image of (g) right hepatic lobe; (h) islets (white spots) in liver reconstructed from the same liver sample as (a). Scale bars indicate 1 mm in (c), (d), (e), (g), and (h) and 300 μ m in (f).

Figure 2. Comparison of the number of islets transplanted with that obtained by OPT analysis.

Representative OPT image of recipient liver transplanted with (a) 75, (b) 150, and (c) 300 islets, respectively. (d) Correlation of the number of islets transplanted and OPT-detected islets. Scale bar indicates 1 mm.

Figure 3. Glycemic level and number of islets of STZ-induced diabetic mice after syngeneic and allogeneic islet transplantation.

(a) Random blood glucose level of recipients (open circles: syngeneic transplantation, filled circles: allogeneic transplantation). (b) Number of transplanted islets in syngeneic and allogeneic transplantation eleven days after transplantation.

Figure 4. Quantitative analysis of transplanted islets in syngeneic and allogeneic model.

(a) Size distribution of transplanted islets. (b) Total volume of transplanted islets in liver obtained by OPT analysis.

Fig. 1

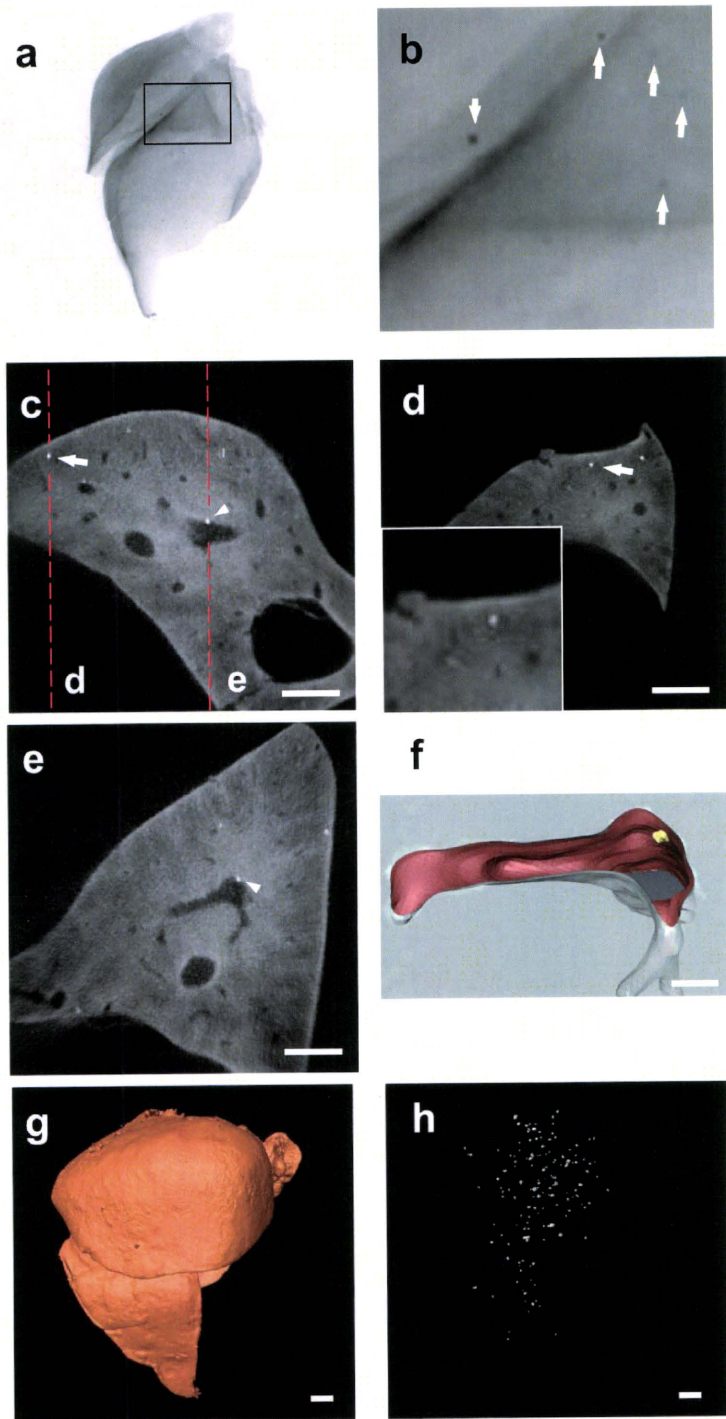


Fig.2

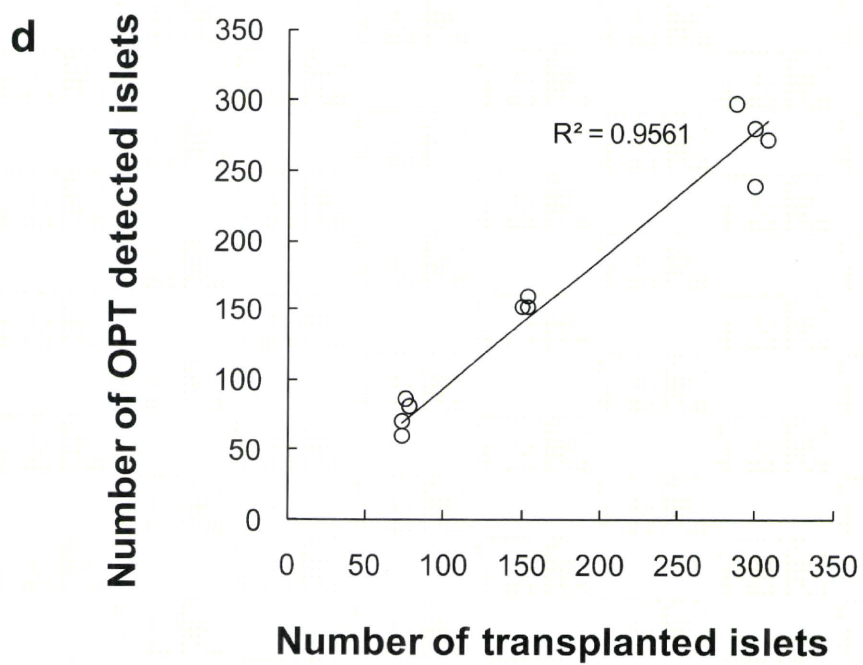
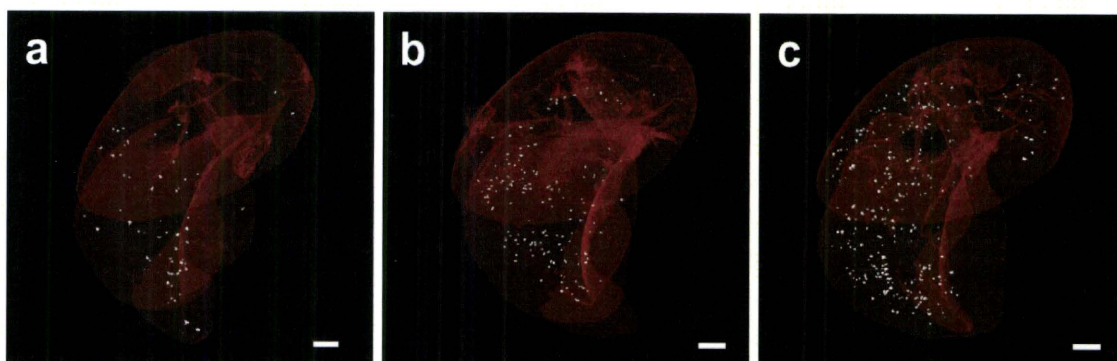


Fig. 3

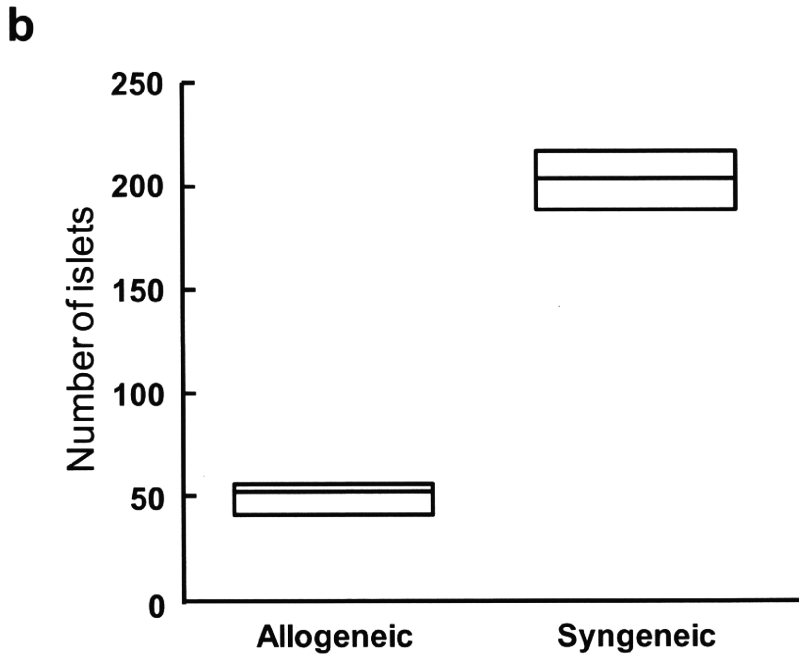
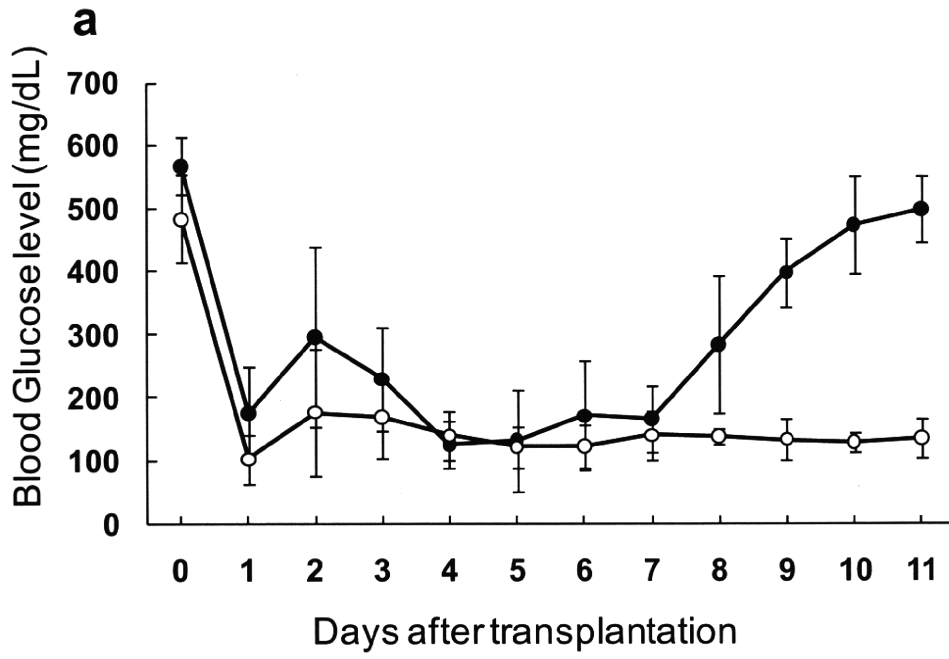
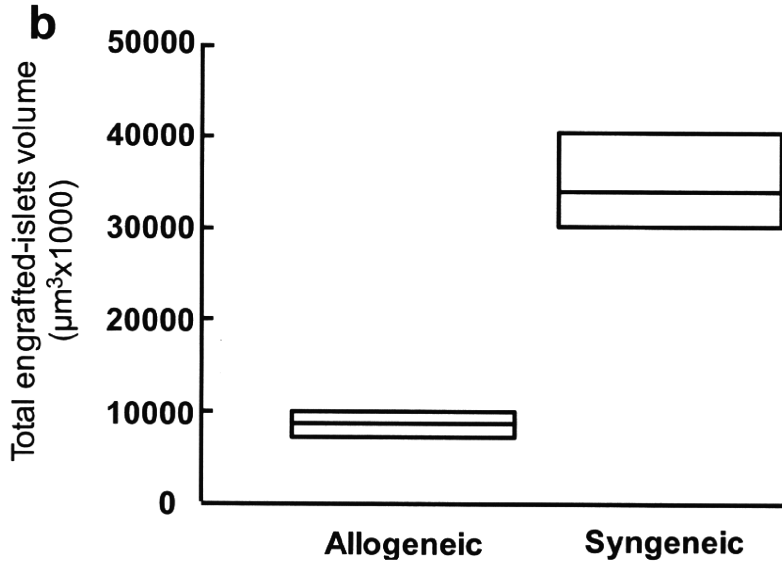
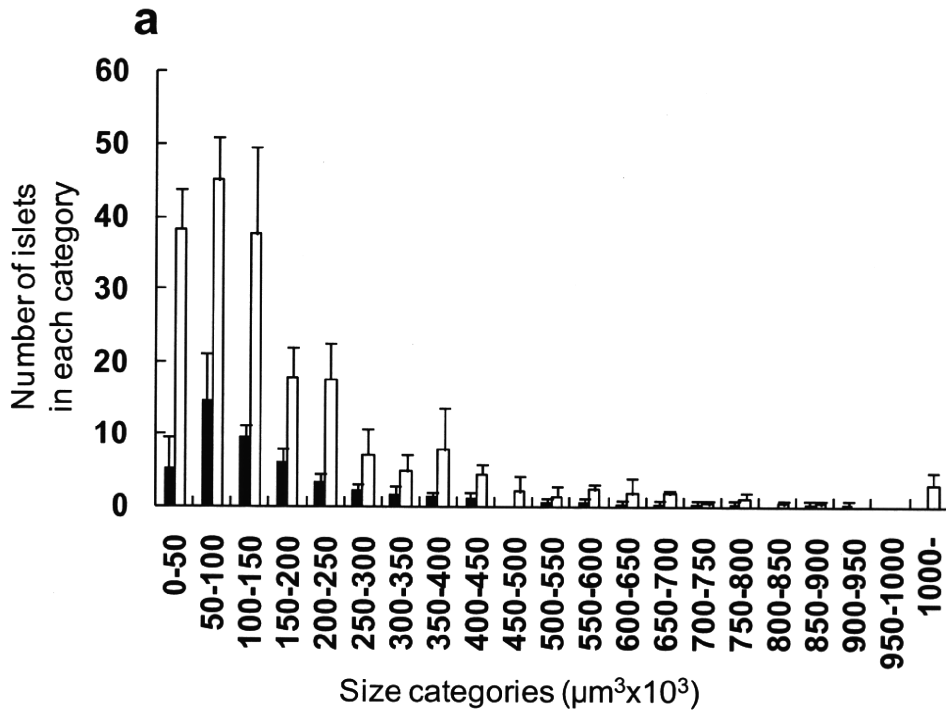


Fig. 4



Relationship of homocysteine and homocysteine-related vitamins to bone mineral density in Japanese patients with type 2 diabetes

Chizumi Yamada¹, Shimpei Fujimoto^{1*}, Kaori Ikeda¹, Yuki Nomura², Ami Matsubara², Miwako Kanno², Kenichiro Shide², Kiyoshi Tanaka³, Eri Imai⁴, Tsutomu Fukuwatari⁴, Katsumi Shibata⁴, Nobuya Inagaki¹

ABSTRACT

Aims/Introduction: To estimate nutritional risk factors for osteoporosis in patients with type 2 diabetes, bone mineral density, homocysteine level, and intakes and levels of Hcy-related vitamins including folate, vitamin B₆ and vitamin B₁₂ were analyzed in a cross-sectional study.

Materials and Methods: Lumbar spine and femoral neck bone mineral density, serum concentrations of vitamin B₆, vitamin B₁₂, and folate and plasma homocysteine levels were measured in 125 Japanese patients with type 2 diabetes. Nutrient intake values were evaluated using a food frequency questionnaire.

Results: Homocysteine was inversely correlated with bone mineral density, and with both dietary intake and serum concentration of folate. Intake of green vegetables was correlated with intake and level of folate and homocysteine levels. When the population was analyzed across the quartiles, bone mineral density, serum folate concentration, folate intake and intake of green vegetables were lowest in the highest homocysteine group.

Conclusions: In patients with type 2 diabetes, the nutritional status of folate might affect the homocysteine level, a putative risk factor for osteoporosis. (*J Diabetes Invest*, doi: 10.1111/j.2040-1124.2010.00088.x, 2010)

KEY WORDS: Osteoporosis, Homocysteine, Folate

INTRODUCTION

Diabetes is becoming increasingly recognized as a risk factor for osteoporotic fracture. Although fracture risk in patients with type 2 diabetes is increased compared with normal subjects, not only in those with low bone mineral density (BMD) but also in those with normal or high BMD^{1–3}, decreased BMD is a major determinant of fragility fracture.

Patients with type 2 diabetes often follow a calorie-restricted diet, but few studies have investigated the sufficiency of these nutrients for the maintenance of skeletal health. Generally, nutrient intake increases along with energy intake. *Ad libitum* food intake values obtained from a longitudinal study in institutionalized elderly found that intake values of vitamins increased along with increased energy intake⁴. In contrast, implementation of a low-fat, low-energy diet (1000 or 1500 kcal/day) in patients with overweight and hyperlipidemia has been shown to

result in a decrease of the intake of certain nutrients, including B-vitamins⁵.

Folate, vitamin B₆ and vitamin B₁₂ are important enzymatic cofactors in the synthesis of methionine from homocysteine (Hcy), and an elevation of Hcy can be caused by insufficiency of folate, vitamin B₆ or vitamin B₁₂. Numerous studies have linked high circulating Hcy levels and low concentrations of folate or vitamin B₁₂ with increased risk of low BMD in non-diabetic subjects^{6–14}. The possibility that elevated Hcy is a risk factor for osteoporosis is suggested by studies of patients with homocystinuria, a rare autosomal recessive disease characterized by markedly elevated levels of plasma Hcy, in which early onset of generalized osteoporosis has occurred^{15,16}. The underlying pathophysiological mechanism of osteoporosis in patients with elevated Hcy is not completely understood. Hcy has been reported to interfere with cross-links of newly formed collagen^{17,18}, and consequently with bone mineralization and strength¹⁹, as well as to stimulate osteoclast formation and activity^{20,21}. However, there has been no report on the association of Hcy and Hcy-related vitamins with osteoporosis in patients with diabetes. Furthermore, vitamin insufficiency was evaluated only by serum vitamin concentrations in most of these studies, and there has been no comprehensive investigation of the relationship of dietary intake of nutrients and

¹Department of Diabetes and Clinical Nutrition, Graduate School of Medicine, Kyoto University, ²Department of Metabolism and Clinical Nutrition, Kyoto University Hospital, Kyoto, ³School of Human Culture, The University of Shiga Prefecture, Hikone, and ⁴Department of Food and Nutrition, Kyoto Women's University, Kyoto, Japan
*Corresponding author. Shimpei Fujimoto Tel.: +81-75-751-3560
Fax: +81-75-751-4244 E-mail address: fujimoto@metab.kuhp.kyoto-u.ac.jp
Received 28 July 2010; revised 8 November 2010; accepted 9 November 2010

serum vitamin concentrations with Hcy and BMD among subjects in the same study.

In the present study, to evaluate nutritional risk factors for osteoporosis in patients with type 2 diabetes, BMD, Hcy level, and intakes and levels of Hcy-related vitamins including folate, vitamin B₆ and vitamin B₁₂ were analyzed.

MATERIALS AND METHODS

Study Population

A total of 125 Japanese patients with type 2 diabetes admitted between December 2008 and June 2009 to Kyoto University Hospital were sequentially enrolled in the study. Lateral lumbar X-ray was carried out to exclude those with scoliosis, compression fractures and ectopic calcifications. Subjects with bilateral hip fractures or prosthesis and other diseases that might influence bone metabolism including liver disease, renal dysfunction (serum creatinine above 2 mg/dL), hyperthyroidism, hyperparathyroidism, hypercorticism, and hypogonadism were excluded. All subjects were free of drugs that influence bone and calcium metabolism including glucocorticoids, bisphosphonates, calcitonin injection, estrogens, selective estrogen receptor modulators, vitamin D, vitamin K, thiazide diuretics, heparin and anticonvulsants. The number of patients treated with thiazolidinedione and metformin was 7 and 28, respectively. The present study was cross-sectional in design, and was approved by The Ethical Committee of Kyoto University Hospital and complies with the Helsinki Declaration. Written informed consent was obtained from all participants.

Measurement of Bone Mineral Density

BMD was measured by dual-energy X-ray absorptiometry (DXA; Discovery; Hologic, Waltham, MA, USA) at the lumbar spine (L1-L4) and femoral neck. The coefficient of variation of the measurements of BMD was 0.39%. BMD (g/cm²) was expressed as Z-score calculated on the basis of the normal reference values of the age- and sex-matched Japanese group provided by the DXA system manufacturer. Because male and female patients of different ages were included in the study, comparison of BMD was made based on Z-scores. Fat mass and lean body mass (without bone mineral content) were measured by DXA (Hologic Discovery; Hologic) using whole-body absorptiometry software, and each value was expressed in kilograms.

Biochemical Measurements

Blood samples were obtained after overnight fasting immediately after admission. Glycosylated hemoglobin (HbA_{1c}) was measured by high performance liquid chromatography (HPLC). The value for HbA_{1c} (%) is estimated as a National Glycohemoglobin Standardization Program (NGSP) equivalent value (%) calculated by the formula $HbA_{1c} (\%) = HbA_{1c} [Japan Diabetes Society (JDS); \%] + 0.4\%$, considering the relational expression of HbA_{1c} (JDS; %) measured by the previous Japanese standard substance and measurement methods and HbA_{1c} (NGSP)²². Fasting serum C-peptide was measured by ELISA (ST AIA-

PACK C-Peptide; Toso Corporation, Tokyo, Japan). Bone-specific alkaline phosphatase (BAP) was measured by enzyme immunoassay (Osteolinks BAP; DS Pharma Biomedical, Suita, Japan), and urine N-terminal cross-linked telopeptide of type-I collagen (uNTx) was measured by ELISA (Osteomark NTx ELISA Urine; Inverness Medical, Waltham, MA, USA). Plasma Hcy levels were determined by HPLC using a thiol-specific fluorogenic reagent, ammonium 7-fluorobenzo-2-oxa-1,3-diazole-4-sulfate²³, and the upper limit of Hcy was 13.5 nmol/L. As pyridoxal 5'-phosphate (PLP) is the predominant circulating form of vitamin B₆, serum PLP concentrations were measured by HPLC^{24,25} for evaluation of vitamin B₆ status. For vitamin B₁₂ measurement, 0.2 mmol/L acetate buffer (pH 4.8) was added to the serum samples, and the vitamin B₁₂ was converted to cyanocobalamin by boiling with 0.0006% potassium cyanide at acidic pH. Cyanocobalamin was determined by the microbioassay method using *Lactobacillus leichmanii*, ATCC 7830^{24,25}. Serum folate was determined by the microbioassay method using *Lactobacillus casei* ATCC 2733^{24,25}.

Evaluation of Dietary Nutrient Intake

A food frequency questionnaire (FFQ) validated by Takahashi *et al.*^{26,27} was used to calculate nutrient intakes. The FFQ used in the present study included questions on the consumption of various food items over the previous 1 or 2 months. Daily nutrient intake was calculated by multiplying the frequency of consumption of each food by the nutrient content of the portion size and summing the products for all food items. The FFQ is validated against 7-day dietary records and the FFQ-estimated nutrient intake values are 72–121% of those of 7-day dietary records²⁶. The reproducibility of the FFQ at intervals of 1–2 months is 93–119% for each nutrient²⁶. Correlations of dietary folate intake, serum folate concentration, and plasma Hcy level with intakes of various food groups including grain/rice, potato, green vegetables, other vegetables, fruits, seaweeds, beans/soy products, seafood, meats, egg, milk products and oil/fat were evaluated.

Statistical Analysis

Data were expressed as mean ± SD. SPSS statistical software (version 13.0; SPSS, Chicago, IL, USA) was used for all statistical analyses. Pearson's correlation coefficient was calculated as a measure of association by adjusting for age and sex where appropriate. Stepwise multiple linear regression analyses were carried out to determine independent factors for plasma Hcy levels including (i) dietary vitamin B₆, vitamin B₁₂ and folate intake values; and (ii) serum PLP, vitamin B₁₂ and folate concentrations as independent variables. The relationship between BMD with Hcy and Hcy-related vitamins was further explored using a quartile-based analysis. Statistical differences among the groups were evaluated using analysis of covariance (ANCOVA) adjusted for age and sex, and Dunnett's multiple comparison tests by comparison with the highest Hcy group. *P* < 0.05 was considered significant.

RESULTS

Clinical characteristics, laboratory data and nutrient intake of subjects are shown in Table 1. The average serum vitamin B₁₂ concentration was 1.45 ± 0.45 pmol/mL (Table 1) and there was no difference between patients taking metformin (1.52 ± 0.49 pmol/mL, $n = 97$) and those without (1.43 ± 0.49 pmol/mL, $n = 28$). Nutrient intake values were significantly positively correlated with total energy intake (Table 2). Dietary vitamin B₆, vitamin B₁₂ and folate intake values were positively correlated with serum vitamin B₆, vitamin B₁₂ and folate levels, respectively (Table 2). Plasma Hcy levels were negatively correlated with both dietary intake and serum concentration of folate (Table 2). Only vitamin B₆ intake and not vitamin B₆ concentration showed a weak negative correlation with Hcy; the influence of vitamin B₁₂ on Hcy elevation was unclear (Table 2). Stepwise multiple linear regression analyses were carried out to

Table 1 | Background characteristics of the study subjects

Characteristic	
No. subjects	125
Male/female	79 (63.2%)/46 (36.8%)
Age (years)	61.2 \pm 12.4
Duration of diabetes (years)	11.2 \pm 9.4
Diabetes treatment	27 (21.6%)/62 (49.6%)
(diet/OHA/Ins/Ins + OHA)	28 (22.4%)/8 (6.4%)
BMI (kg/m ²)	24.9 \pm 4.9
Fat mass (kg)	16.5 \pm 9.8
Lean body mass (kg)	45.9 \pm 9.3
Fasting plasma glucose (mg/dL)	160.2 \pm 48.6
HbA _{1c} (%)	9.6 \pm 2.2
Fasting serum C-peptide (ng/mL)	1.71 \pm 0.89
Serum BAP (U/L)	23.5 \pm 8.7
uNTx (nMBCE/mmol Cr)	35.6 \pm 19.8
Energy intake (kcal/day)	2073.2 \pm 582.5
Protein/fat/carbohydrate	73.6 \pm 19.7/64.4 \pm 23.7/
intake (g/day)	278.7 \pm 80.2
Calcium intake (mg/day)	596.0 \pm 213.6
Vitamin D intake (μ g/day)	9.21 \pm 4.48
Vitamin B ₆ intake (mg/day)	1.22 \pm 0.34
Vitamin B ₁₂ intake (μ g/day)	8.81 \pm 4.65
Folate intake (μ g/day)	287.4 \pm 100.5
Serum PLP concentration	61.3 \pm 29.1
(pmol/mL)	
Serum vitamin B ₁₂	1.45 \pm 0.45
concentration (pmol/mL)	
Serum folate concentration	27.5 \pm 10.3
(pmol/mL)	
Plasma homocysteine	11.2 \pm 5.1
concentration (nmol/mL)	

Data are number of patients (categorized data) or mean \pm SD (quantitative data).

BAP, bone-specific alkaline phosphatase; BMI, body mass index; Ins, insulin; OHA, oral hypoglycemic agents; PLP, pyridoxal 5'-phosphate; uNTX, urine N-terminal cross-linked telopeptide of type-I collagen.

Table 2 | Correlations among dietary nutrient intake values, serum concentrations and plasma homocysteine levels adjusted for age and sex

	<i>r</i>	<i>P</i>
Correlations of total energy intake with various nutrient intakes		
Vitamin B ₆ (mg)	0.521	<0.001
Vitamin B ₁₂ (μ g)	0.253	0.005
Folate (μ g)	0.331	<0.001
Correlations of intake values with serum concentrations		
Vitamin B ₆	0.192	0.034
Vitamin B ₁₂	0.336	<0.001
Folate	0.400	<0.001
Correlations of plasma Hcy levels with B vitamins		
Vitamin B ₆ intake (mg)	-0.207	0.022
Vitamin B ₁₂ intake (μ g)	-0.001	0.988
Folate intake (μ g)	-0.328	<0.001
Serum PLP concentration (pmol/mL)	0.002	0.982
Serum B ₁₂ concentration (pmol/mL)	0.001	0.993
Serum folate concentration (pmol/mL)	-0.369	<0.001

Hcy, homocysteine; PLP, pyridoxal 5'-phosphate.

determine independent factors for plasma Hcy levels. Dietary folate intake was a significant predictor of Hcy when dietary vitamin B₆, vitamin B₁₂ and folate intake values were included as independent variables ($R^2 = 0.088$, β -coefficient = -0.297 , $P < 0.001$), and serum folate concentration also was a significant predictor of Hcy when serum PLP, vitamin B₁₂ and folate concentrations were included as independent variables ($R^2 = 0.121$, β -coefficient = -0.347 , $P < 0.001$). We then evaluated the correlations of folate intake and the concentrations of folate and Hcy with intake of the various food groups determined by FFQ. Dietary folate intake and serum folate concentration were significantly associated with intakes of certain food groups including potato, green vegetables, other vegetables and fruits. Only intake of green vegetables was significantly correlated with the plasma Hcy level (Table 3).

Bone mineral density of lumbar spine (SP-BMD) and femoral neck (FN-BMD) were positively correlated with body mass index (BMI) and fat mass, although no significant correlations were found in diabetes-related parameters including fasting plasma glucose, HbA_{1c} and diabetes duration (Table 4). Both SP-BMD and FN-BMD were positively correlated with fasting serum C-peptide, but these correlations were cancelled when adjusted for BMI. Urinary NTx, a marker of bone resorption, was negatively correlated with FN-BMD. As nutrient intake significantly increases with energy intake, nutrition intakes were also evaluated by adjusting for calories. As a result, calorie-adjusted folate intake was positively correlated with SP-BMD, although the association between calorie-adjusted folate and FN-BMD did not reach statistical significance. There were no significant associations between BMD of both sites and serum concentrations of vitamin B₆, vitamin B₁₂ and folate. The plasma Hcy concentration was negatively correlated with both